Available online at www.sciencedirect.com
ScienceDirect
Nuclear Instruments and Methods in Physics Research A 586 (2008) 300–308
NUCLEAR INSTRUMENTS & METHODS IN PHYSICS RESEARCH Section A
www.elsevier.com/locate/nima

Wavelength shifter strips and G-APD arrays for the read-out of the z-coordinate in axial PET modules

A. Braem[a], E. Chesi[a], C. Joram[a,*], A. Rudge[a], J. Séguinot[a], P. Weilhammer[a,1], R. De Leo[b], E. Nappi[b], W. Lustermann[c], D. Schinzel[c], I. Johnson[d], D. Renker[d], S. Albrecht[e]

[a]*CERN, PH Department, CH-1211 Geneva, Switzerland*
[b]*INFN, Sezione di Bari, I-70122 Bari, Italy*
[c]*ETH Zürich, CH-8092 Zürich, Switzerland*
[d]*Paul Scherrer Institut, CH-5232 Villigen, Switzerland*
[e]*University Hospital Geneva, CH-1211 Geneva, Switzerland*

Received 1 November 2007; received in revised form 14 November 2007; accepted 14 November 2007
Available online 24 November 2007

Abstract

The measurements presented in this paper are related to the development of a PET camera based on a 3-D axial geometry with excellent 3-D spatial, timing and energy resolution. The detector modules consist of matrices of long axially oriented scintillation crystal bars, which are individually coupled to photodetectors. The axial coordinate is derived from wavelength shifting (WLS) plastic strips orthogonally interleaved between the crystal bars and readout by G-APD arrays. We report on results from measurements with two LYSO crystal bars, read with PMTs, and two WLS strips readout with G-APD devices from Hamamatsu (called MPPC). The WLS strips are positioned orthogonally underneath the LYSO bars. Yields of about 80 photoelectrons from the WLS strips for an energy deposition in the LYSO crystals equivalent to the absorption of 511 keV photons are observed. The axial coordinate in the LYSO bars is reconstructed with a precision of about 1.9 mm (FWHM) using a digital reconstruction method. The resolution of an analog coordinate reconstruction method, which uses the pulse height measurement from the WLS strips is 2.8 mm (FWHM). This resolution is still compromised by the availability of only two WLS strips and will improve with a full stack of LYSO crystals interleaved with WLS strip arrays, which is presently under development for a PET demonstrator set-up.

PACS: 87.58.Fg; 85.60.Ha; 85.40.−e

Keywords: PET; Axial geometry; Scintillator; LYSO; Wavelength shifter; G-APD

1. Introduction

The concept of a brain PET scanner module with axially arranged scintillation crystals has been described in detail in a previous publication [1]. This approach offers substantial advantages in performance compared with existing instruments. The main improvements in the new concept are true 3-D coordinate reconstruction of the 511 keV photon interaction and therefore no depth-of-interaction (DOI) uncertainty, improved spatial resolution and high detection efficiency, uniformity of spatial resolution over the complete field of view, and capability to identify photon interactions with Compton cascades.

In a recent article [2] we demonstrated the potential of wavelength shifting (WLS) strips to readout the axial z-coordinate of a γ interacting in long LYSO crystal bars ($3.2 \times 3.2 \times 100\,\mathrm{mm}^3$). However, in this work the strips were read out with conventional PMTs which would make it very difficult to realize large matrices of close crystal bars because of packaging constraints.

In the present article we describe and discuss measurements using instead G-APD arrays to read out the

*Corresponding author.
E-mail address: Christian.Joram@cern.ch (C. Joram).
[1]Also affiliated to University/INFN Perugia, I-06100 Perugia, Italy.

0168-9002/$ - see front matter © 2007 Elsevier B.V. All rights reserved.
doi:10.1016/j.nima.2007.11.022

WLS-strips. Thanks to their immunity to magnetic fields, the use of G-APDs for the readout of both crystals and WLS strips opens up the possibility of simultaneous co-registration of the PET data with MRI.

The G-APDs have a quantum efficiency QE of ~30%, about twice the QE of PMTs at 490 nm wavelength, the emission peak of green WLS, which allows to obtain high detection efficiency, even for low energy recoil electrons from Compton interactions. Moreover, because of their size and geometric detection efficiency, G-APD arrays match the limited available space imposed by the design of matrices with closely stacked scintillating crystal bars [1].

We describe in detail the principle of the measurements based on a *pulsed low energy electron beam*, the test set-up and the optical properties and characteristics of its components. Unfortunately only two G-APDs were available for these measurements. The crystal bars were therefore read with a conventional PMT. From the test results, we deduce the achievable photon yields of the LYSO crystal bars and of the WLS-strips, parameters which determine the achievable energy resolution and the spatial reconstruction of the 3-D axial PET concept. We then present the performance obtained with a digital and an analog axial z-reconstruction method and compare it with MC simulations.

The low energy range is of particular interest for the 3-D axial camera concept in order to unambiguously discriminate and precisely reconstruct Compton interactions in LYSO crystal matrices. Therefore, the tests were performed in the energy interval of 50–300 keV. Above this interval, up to the photoelectric peak of the 511 keV γ ray, the photon yield of the LYSO bars and WLS-strips can be linearly extrapolated as previously demonstrated [2]. We also present measurements with a modified set-up where we read a LYSO crystal bar with a G-APD at energies up to 534 keV.

2. Experimental principle and set-up

In order to vary the energy deposition and its position along the LYSO crystal bars in an easily controllable way, we used a *pulsed and narrow low energy electron beam* (Fig. 1) which impinges at normal incidence the surface of the crystals. The electrons are generated by illuminating a semi-transparent CsI photocathode of 10 nm thickness, vacuum deposited on a gold mesh (optical transparency T~0.90) printed on a CaF_2 crystal disk, with short (~10 ns) UV light pulses. The light source, a self triggered H_2 flash lamp ($\lambda_{peak} = 160$ nm), is collimated in such a way that the light spot at the level of the photocathode has a Gaussian shape of 1.8 mm FWHM in both transversal coordinates (x, z).

A negative potential ($10\,kV \leqslant U_{acc} \leqslant 30\,kV$) is applied between the gold mesh underneath the CsI photocathode and a metallic transparent mesh ($T > 0.95$) at ground potential, mounted 0.5 mm above the LYSO bars. This configuration ensures a uniform parallel electric field which

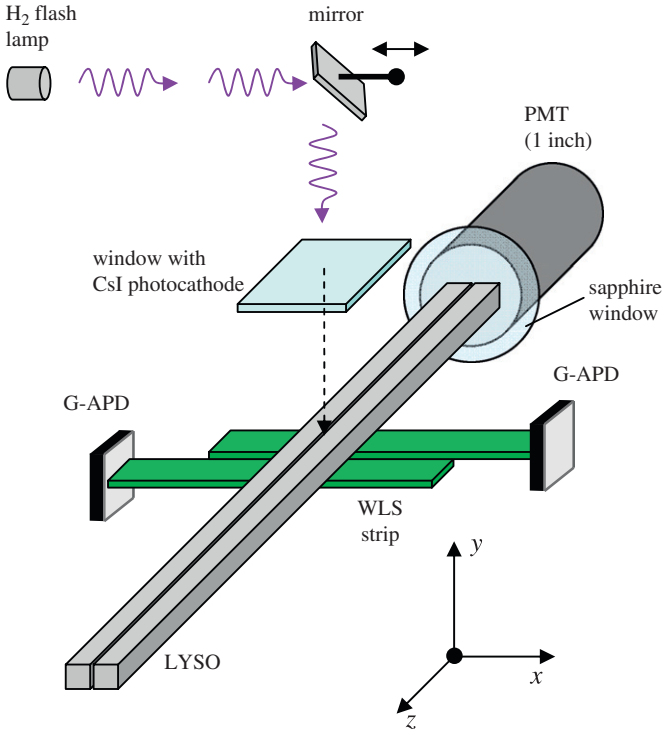

Fig. 1. Concept and schematic representation of the set-up.

defines the kinetic energy of the accelerated electrons when they hit the crystals. Apart from the transverse point spread (~0.3 mm) the electron beam spot size is preserved from the photocathode to impact plane.

The set-up allows (1) a precise adjustment of the energy deposited by controlling the number of photoelectrons N_{pe} emitted from the photocathode and the acceleration voltage U_{acc}, and (2) the scanning of the crystal surface by accurately displacing the light spot by means of a mirror indicated in Fig. 1.

The measurements were performed in vacuum at a pressure of a few 10^{-6} mbar.

2.1. Description of the set-up

The test set-up comprises two closed optically polished LYSO:Ce crystals[2] ($3.2 \times 3.2 \times 100\,mm^3$) mounted side by side with one of their end faces optically coupled through a vacuum tight thin (1 mm) sapphire window to a single PMT.[3] The opposite end faces of the bars are mirror coated with a vacuum evaporated Al film.

Two 60 mm long WLS strips[4] of $3 \times 1.1\,mm^2$ cross-section were mounted orthogonal and underneath the two LYSO crystals with a small gap. Each WLS strip was readout at opposite sides by a G-APD array from Hamamatsu[5] (MPPC[6] type S 10362-33-050 C) with

[2]Saint-Gobain Crystals, Nemours, France.
[3]XP3102, Photonis. Brive-La Gaillarde, France.
[4]EJ-280-10 ×, ELJEN Technology, Sweetwater, TX, USA.
[5]Hamamatsu Photonics K.K., Hamamatsu City, Japan.
[6]MPPC = Multi Pixel Photon Counter.

$3 \times 3\,mm^2$ active area. The strip end opposite to the MPPC was coated with a reflective Al film. Moreover, a thin Al foil underneath the WLS-strips reflects the small fraction of the non-absorbed light back onto the strips. This doubles the total light path of the LYSO scintillation in the WLS strip and hence increases the absorption probability. Standard optical grease was used to improve the light transmission with the photon detectors (PMT and MPPC).

The signals from the MPPCs were amplified by a factor 30, for matching to the readout electronics, with a fast voltage amplifier[7] ($\Delta B = 150\,MHz$, $50\,\Omega$ input impedance, $600\,\mu V$ RMS output noise) located inside the vacuum enclosure and close to the MPPC.

The waveforms from the LYSO/PMT and the WLS strips/MPPCs were integrated and readout by a 16 channels charge sensitive ADC[8] module. A common gate, allowing an effective integration over about 3 times the LYSO decay time, was applied to the ADC module synchronously with the electron beam pulse.

The ADC module was readout with a VME-DAQ system interfaced to a PC via an interface CAEN V1778. Histograms and fits to the data were performed using the standard CERN subroutines HBOOK and PAW.

2.2. Characterization of the components

2.2.1. Physical properties and characterization of the WLS strips

The absorption peak of the ELJEN WLS plastic EJ-280 is centered at 425 nm, wavelength of the scintillation emission peak of LYSO crystals. The density of the plastic material is $1.02\,g/cm^3$ and its refractive index is 1.58. The fluorescent light of the plastic is shifted into the green range with a peak emission at 490 nm. The quantum efficiency of the fluorescent dye is 0.86 and its decay time 8.5 ns according to the manufacturer characteristics.

For our application, on request, ELJEN produced WLS sheets ($10 \times 10\,cm^2$) of three different thickness ($d_{strip} = 0.7,\ 1.1,\ 1.5\,mm$) with a dye concentration 10 times higher than their standard material in order to enhance the light absorption coefficient.

As illustration, Fig. 2 shows a measurement of the transmission coefficient versus the wavelength, performed with a spectro-photometer,[9] for the three plastic sheet thicknesses. At 425 nm the three measurements are compatible with an absorption coefficient of $2.5\,mm^{-1}$. By using a reflector below the WLS strips as described above, more than 80% of the light entering the 0.7 mm thick strip can be absorbed.

WLS strips of $3 \times 60 \times d_{strip}\,mm^3$ were produced by cutting the plastic sheets with a diamond saw and polishing the machined surfaces to a standard optical quality. In Fig. 3 the relative light yield was measured as a function of the distance to the readout PMT using a blue LED light source to excite the WLS material. The green light, isotropically emitted, is propagated to both ends of the strips by total internal reflection. For this specific measurement, the end face of the strip opposite to the PMT was not Al coated. The results indicate that the relative light yield at one end, without Al coating at the opposite end, is 78–88% for a distance of 3 cm (half the strip length) from the PMT and for a thickness of 0.7 and 1.1 mm, respectively. The attenuation length is enhanced by a factor of ~2 going from a strip thickness of 0.7–1.5 mm. The difference of the light yield at $z = 0$ reflects the difference of the light absorption. During these tests it was noted that

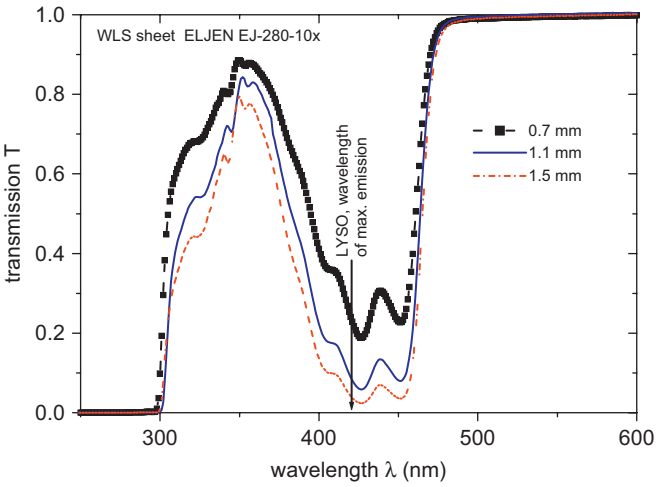

Fig. 2. Measured transmission coefficient for three sheets of high concentration WLS materials (0.7, 1.1 and 1.5 mm thick). The data are corrected for the Fresnel reflections at the sheet/air interfaces. The corresponding absorption coefficient in the wavelength band 400–460 nm is around $2\,mm^{-1}$.

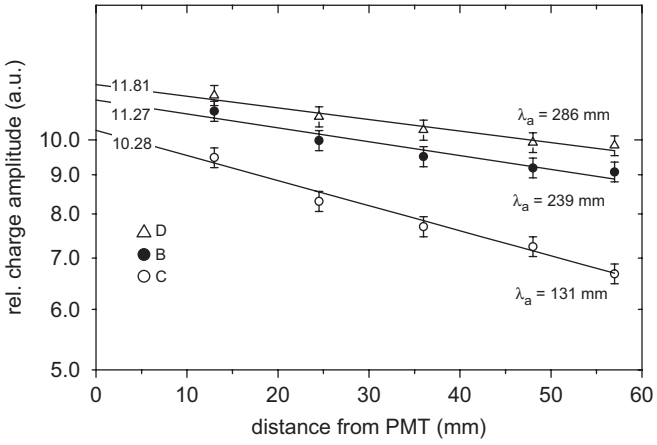

Fig. 3. Light absorption in WLS strips of 0.7, 1.1 and 1.5 mm thickness. The plot shows the relative light output measured with a PMT at $z = 0$ as a function of the distance from the emission point. The data are fitted with exponentials yielding the absorption lengths $\lambda_a = 131$, 239 and 287 mm.

[7]OPA847 from Burr-Brown/Texas Instruments, TX, USA, configured as a voltage amplifier with a gain of 30.

[8]VME module Lecroy 1182 (50 fC/ADC count sensitivity).

[9]Perkin-Elmer, type Lambda 15.

the light attenuation length is, as expected, very sensitive to the surface quality of all faces of the strip.

2.2.2. Characterization of the MPPC

The MPPCs from Hamamatsu, type S 10362-33-050 C, are Geiger-APD devices comprising 3600 pixels of $50 \times 50\,\mu m^2$ covering a total area $3 \times 3\,mm^2$ with a geometric efficiency of 61.5%. Following the specifications of the manufacturer the QE is about 35% at 400 nm for an avalanche gain of 5.7×10^5. This value includes the optical cross-talk and the after pulses contributions.

Prior to the tests we have measured the performance of the MPPCs in the conditions of their use, i.e. with a coupling to a fast voltage amplifier as described above. These measurements performed by using a pulsed blue LED as light source are essential to correctly estimate the photoelectron yield of the WLS strips.

Fig. 4 shows the results obtained at a temperature of 26 °C for one of the MPPCs. Apart from an offset in the operating voltage both devices used show very similar characteristics. Fig. 4 (left) displays the variations of the gain with the applied voltage, the dark rate and the optical cross-talk effect. Fig. 4 (right) shows the efficiency to detect one or more photoelectrons as a function of the bias voltage. The efficiency ε is derived from the Poisson probability $P(0)$ to measure 0 photoelectrons while on average μ photoelectrons are detected: $\varepsilon = 1-P(0) = 1-e^{-\mu}$. The value attained on the plateau indicated that the light intensity of the blue LED was adjusted so that a mean value of $\mu = 1.9$ p.e. was detected. The measurements show that for this MPPC an operational voltage around −71 V allows an efficient single photon detection efficiency at a gain of 3.5×10^5 with a dark rate of the order of 2.5 MHz and an optical cross-talk of about 18%. For the following measurements the operational voltage was set to −71.2 V.

We plan to use G-APD devices of $3 \times 1.2\,mm^2$ effective area to realize in a next step a demonstrator module consisting of two LYSO crystal stacks of 40 crystal bars each.

2.3. Electron beam energy

For a relatively small number of electrons (<30) the fluctuation $\sigma(N_e) = \sqrt{N_e}$ dominates the charge distribution measured at the output of the LYSO/PMT over the photoelectron statistic of the detected scintillation light. This is illustrated in Fig. 5 which displays, as an example, the charge distribution Q obtained at $U_{acc} = 25$ kV. The mean number of electrons N_e per bunch which defines the deposited energy is determined from the relation

$$N_e = \mathrm{ENF}(\langle Q\rangle/\sigma_Q)^2 \quad (1)$$

with $\langle Q\rangle$ and σ_Q being the mean value of the charge distribution and its variance, respectively. ENF is the excess noise factor of the PMT (ENF∼1.1 was derived from the peak-to-valley ratio of this PMT for single photons). The mean deposited energy per bunch is

$$E_d = eN_eU_{acc}. \quad (2)$$

Fig. 5 shows, as an example, a charge spectrum (before pedestal subtraction) taken at an acceleration voltage of 25 kV. The analysis leads to a mean number of electrons in the bunch of $N_e = 10$.

However, the deposited energy, which is finally converted to scintillation light is reduced by two well-known low-energy effects: (1) a fraction (∼45%) of the electrons is back scattered from the crystals without depositing their

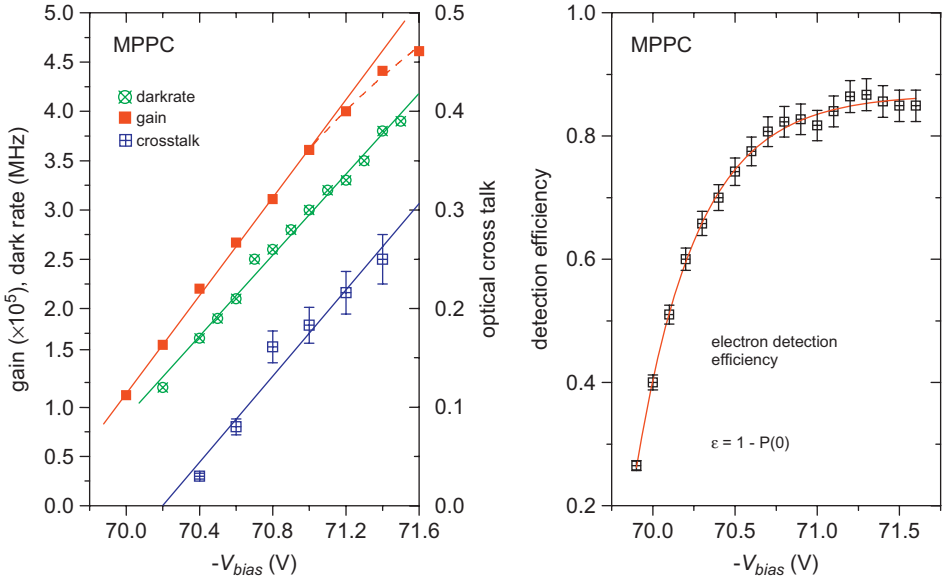

Fig. 4. Properties of the Hamamatsu MPPC 33-050C. Left: Charge gain, dark count rate and optical cross-talk are plotted as function of the applied bias voltage. Right: The detection efficiency ε for $\geqslant 1$ photoelectron, obtained from the 'zero' count rate, is plotted versus the bias voltage.

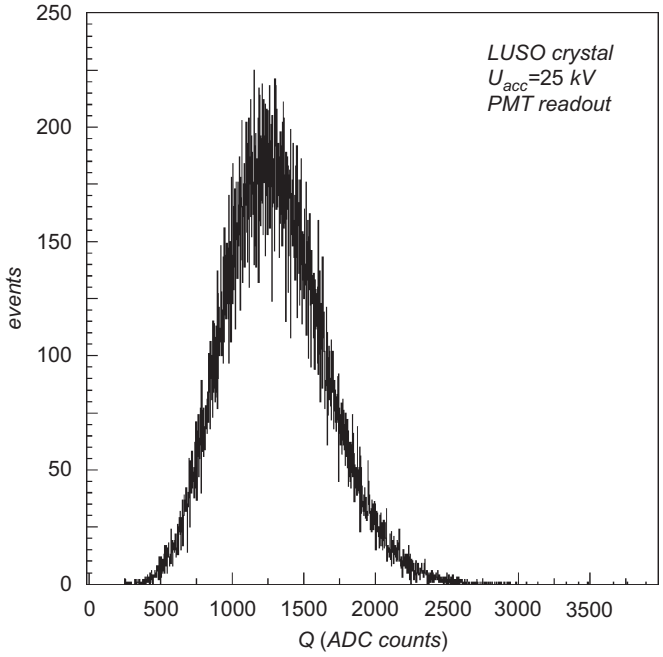

Fig. 5. Example of a charge spectrum (1 ADC count = 50 fC). The LYSO crystal bars were bombarded with bunches of on average 10 electrons. The acceleration voltage was set to 25 kV. The mean and RMS value of the distribution are 1305 and 350.5 ADC counts, respectively.

full energy [3], (2) the light yield of the LYSO crystal at low energies (up to ~100 keV) is not linear with the deposited energy. The latter effect is described by the so-called Relative Light Output (RLO). For LSO crystals RLO values of 0.8 have been measured for an energy deposition of 25 keV [4]. They approach 1 for depositions above 50 keV.

We take into account both effects by introducing a parameter κ which depends on the acceleration voltage U_{acc}. An electron bunch of energy $eN_{\mathrm{e}}U_{\mathrm{acc}}$ hitting the crystal leads to an amount of energy E_{c} which is actually converted to scintillation photons

$$E_{\mathrm{c}} = eN_{\mathrm{e}}U_{\mathrm{acc}}\kappa(U_{\mathrm{acc}}). \tag{3}$$

No RLO data are available for LYSO. Assuming that LYSO shows the same RLO characteristics as LSO, we calculate the parameter $\kappa(U_{\mathrm{acc}})$ with a simple Monte-Carlo (MC) program. Alternatively, as will be discussed below, we are able to extract $\kappa(U_{\mathrm{acc}})$ for LYSO in a linear approximation directly from our measurements.

For γ rays, in contrast to low energy electrons, there is no back scattering effect and above about 100 keV the RLO is essentially 100%. The deposited and converted energy are therefore identical.

2.4. Determination of photoelectron yield of the LYSO crystal bars

The photoelectron yield obtained at the ends of long LYSO crystal bars with all faces optically polished has been shown to vary exponentially with the path length of the scintillation light [5]. In our test set-up the two crystals are coupled to a single photon detector (PMT). The total number of detected photoelectrons N_{pe}, at a given converted energy E_{c}, is

$$N_{\mathrm{pe}}(E_{\mathrm{c}}) = \frac{N_0(E_{\mathrm{c}})}{2}[\exp(-z/\lambda_{\mathrm{eff}}) + R\,\exp -((2L_{\mathrm{c}} - z)/\lambda_{\mathrm{eff}})]. \tag{4}$$

The distance z from the emission point to the PMT is about ~7 cm, the length of the bar L_{c} is 10 cm and R is the reflectivity of the aluminum coated end of the crystal bar ($R = 0.8$). λ_{eff} is the effective light absorption length during the propagation which was measured [5] to be close to 40 cm. The parameter N_0 is used to characterize the LYSO bars in absence of light absorption during the propagation of the photons from the emission point to the photodetector. N_0 is equal to the scintillation photon yield multiplied with the fraction of the scintillation light which is propagated in the bar by total internal reflection (typically $\Delta\Omega/4\pi$~60% [1]) and the QE of the PMT (~30% at 420 nm according to the manufacturer's data sheet). N_0 is therefore directly proportional to E_{c}. Inserting these parameters one can calculate from Eq. (4) the number of detected photoelectrons

$$N_{\mathrm{pe}}(E_{\mathrm{c}}) = 0.71N_0(E_{\mathrm{c}}) \tag{5}$$

where E_{c} is the (mean) converted energy as calculated from relation 3.

In the following we derive the parameter N_0 of the LYSO bars for a converted energy E_{c} of 511 keV. The number of photoelectrons $N_{\mathrm{pe}}(E_{\mathrm{c}})$ is calculated from the mean value of the measured PMT charge distribution $\langle Q(E_{\mathrm{c}})\rangle$ (in ADC count), the sensitivity of the ADC (50 fC/ADC count), and the signal attenuation (18 db) which was needed to fit the ADC range,

$$N_{\mathrm{pe}}(E_{\mathrm{c}}) = 8 \times 50 \times 10^{-15}\langle Q(E_{\mathrm{c}})\rangle/(1.6 \times 10^{-19}\,G_{\mathrm{PMT}}). \tag{6}$$

The PMT gain $G_{\mathrm{PMT}} = 5.8 \times 10^6$ was measured at the operating voltage of 1 kV. It follows

$$N_{\mathrm{pe}}(E_{\mathrm{c}}) = 0.431\langle Q(E_{\mathrm{c}})\rangle. \tag{7}$$

3. Experimental results

The main objectives of this study are

1. The experimental proof that the light output of the WLS strips is sufficient to observe the light created not only by the absorption of 511 keV γ rays but also by Compton recoil electrons in the LYSO crystals down to ~50–100 keV.
2. The measurement of the resolution of the digital z-coordinate reconstruction. We also assess the potential of an analog z reconstruction.

3.1. Photoelectron yield of the LYSO crystal bars

Observing the waveforms from the PMT directly on the scope reveals the exponential decay of the scintillation light LYSO:Ce crystals with a time constant of about 30 ns (cf. Fig. 6 in [6]).

Fig. 6 (left) shows the variation of the mean detected charge $\langle Q \rangle$ in ADC counts with the acceleration potential U_{acc} for $N_e = 9.7 \pm 0.5$ beam electrons per bunch. A linear fit to the data indicates that the minimum energy for the electrons to produce scintillation light in the crystals is 3.3 keV.

After converting the measured charge to number of photoelectrons (Eq. (7)), the same data are represented in the right-hand side plot of Fig. 7 in a different way: The photoelectron yield is now plotted versus the converted energy E_c, calculated according to Eq. (3). The parameter $\kappa(U_{acc})$ has been determined in two different ways: (1) from the MC (using measured RLO data for LSO), and (2) by fitting κ in a linear approximation $\kappa(U_{acc}) = a + bU_{acc}$ such that the photoelectron yield can be described as $N_{pe} = cE_c$. The fit leads to $\kappa(U_{acc}) = 0.501 + 0.0117U_{acc}$. The two methods to determine κ differ on average by only 4%.

For a 511 keV γ, one would expect to detect 1050 ± 20 photoelectrons corresponding to a N_0 (511 keV) value of the LYSO crystal bars of 1050/0.71∼1480 (see Eq. (5)). This value is in good agreement with the value of N_0 (511 keV) = 1173 photoelectrons directly measured with 511 keV γ's [7] if one takes into account the different QE values of the PMTs: 30% now compared to 24% in Ref. [7].

Under the assumption of an intrinsic LYSO energy resolution of 7% (FWHM), a photoelectron yield of 1050 at 511 keV is expected to lead to an energy resolution of ∼11% (FWHM), in agreement with our previous measurement [2].

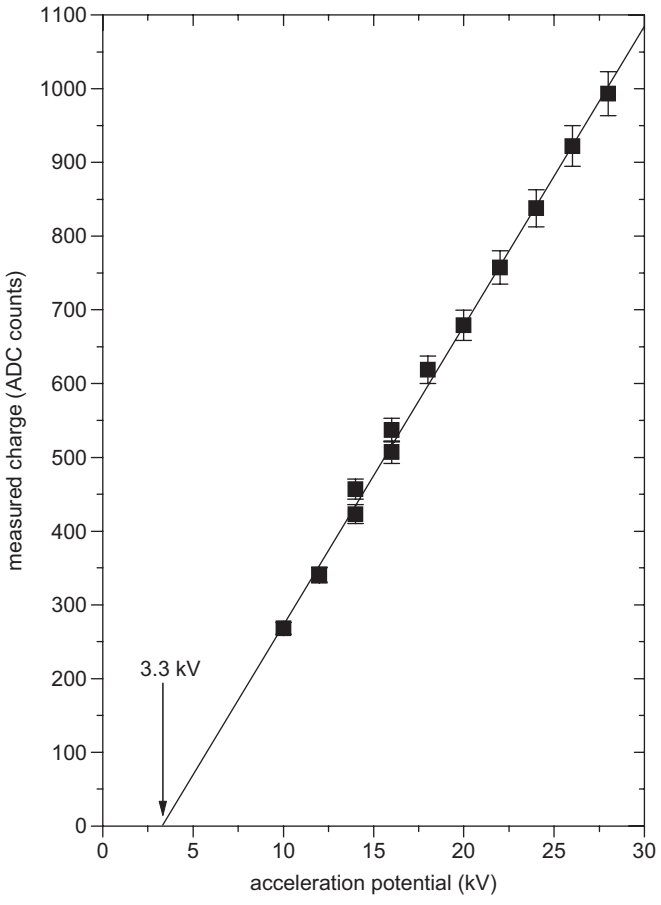

Fig. 6. LYSO bar. Variation of the charge $\langle Q \rangle$ (in ADC counts. 50 fC/count) with the applied acceleration potential.

3.2. Performance of the WLS-strip readout

3.2.1. Photoelectron yield

The gain of the MPPCs was adjusted to 4×10^5 providing a total gain of the readout chain of 12×10^6 including the gain of the serial fast amplifier. The gain of the MPPC was chosen to ensure high detection efficiency for single photons, as discussed in Section 2.2.2.

Fig. 7 (right) shows the sum of the number of detected photoelectrons in the two WLS strips as a function of the converted energy. As for the LYSO bars, the photoelectron yield in the strips varies linearly with the converted energy. At $E_c = 200$ keV a yield of 39 ± 2 is measured, which extrapolates to about 100 photoelectrons for 511 keV γ rays. Correcting for the optical cross-talk of the MPPCs (∼20%), the effective number of detected photons from the WLS strips is estimated to be about 80. This characteristic is expected to ensure high detection efficiency also for the reconstruction of Compton recoil electrons in the energy range of 50–100 keV.

Fig. 8 shows the profiles of the number of detected photoelectrons in a scan of the light spot transverse to the WLS-strips, i.e. along the LYSO crystals. The shown data were obtained at $U_{acc} = 25$ kV for a mean converted energy of $E_c = 200 \pm 12$ keV.

Fig. 8 (left) shows the profile of the number of detected photoelectrons by each strip and Fig. 8 (right) the sum of both strips. The width covered by the strips (approximately $-3 < z_{mir} < 3$ mm) is indicated on the figures.

The large width of the distributions in Fig. 8 (left) of 6–7 mm (FWHM) is due to several contributions: (1) the size of the electron beam spot (1.8 mm FWHM at the photocathode), (2) the point spread from the cathode to the crystals (∼1.2 mm FWHM) and (3) the aperture of the scintillation light emission cone (∼33° in the crystals, 38° in the WLS strips) which escapes the crystals. As the electrons are absorbed in the crystals within a depth of a few micrometer from the surface, the observed width corresponds in practice always to the expansion of the light cone over the full thickness (crystal + WLS). For γ rays randomly absorbed in depth, the average width of the distributions predicted by MC simulations is about 2 mm (FWHM). Therefore, generally one or two strips would be hit, which might allow to improve by interpolation the resolution $\sigma(z)$ of the axial z reconstruction (see below).

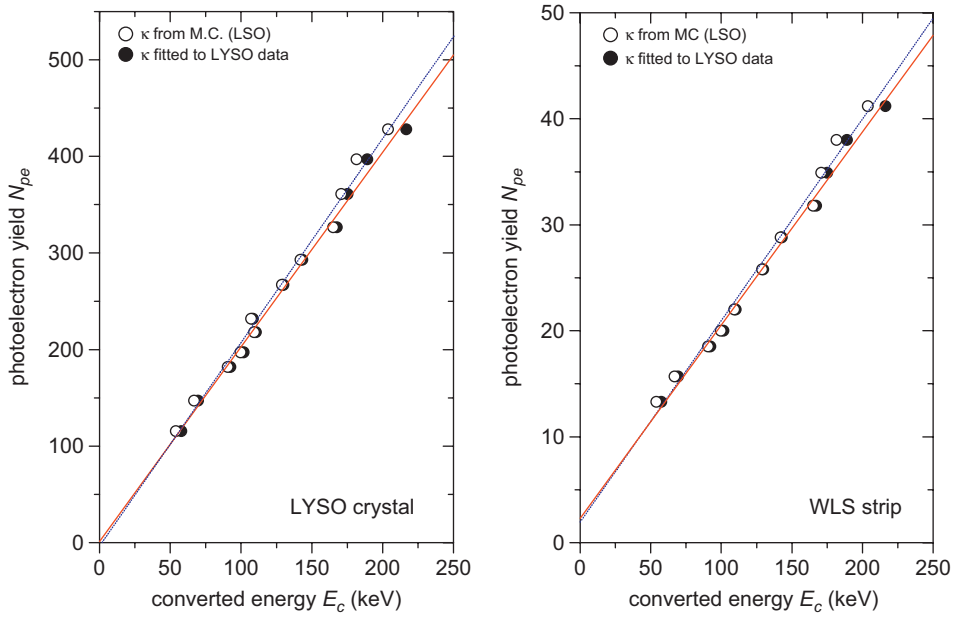

Fig. 7. Readout of the LYSO bars (left) and WLS strips (right). The plots show the dependence of the number of detected photoelectrons on the converted energy.

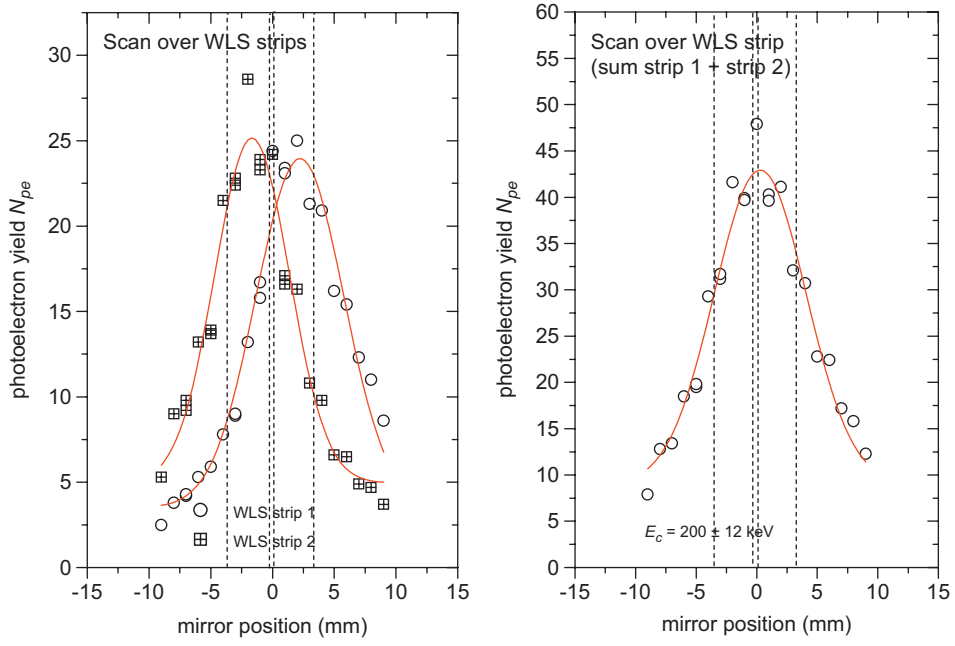

Fig. 8. Photoelectric yield during the scan over the WLS strips. Left: Yield of the individual strips. Right: Sum of the strips. The dashed vertical lines indicate the approximate position of the strips.

3.3. Determination of the axial z-coordinate and precision of the reconstruction

3.3.1. Digital z-reconstruction

To perform the reconstruction several selected discrimination thresholds were applied by software to the charge read out from the strips. If a signal is detected from both strips the reconstructed z-coordinate is assumed in between the two strips ($z_{\mathrm{rec}} = 0$). Otherwise, if only one of the strips is fired, the z-coordinate is reconstructed in the center of the hit strip ($z_{\mathrm{rec}} = -1.5$ or $+1.5$ mm).

For a given z_{mir} position of the mirror, the z_{rec} coordinate in Figs. 9 and 10 is determined from the mean value of the experimental distribution, and the resolution from the RMS value of the distribution. The measured RMS values are in the range of 0.7–0.9 mm in good agreement with MC simulations.

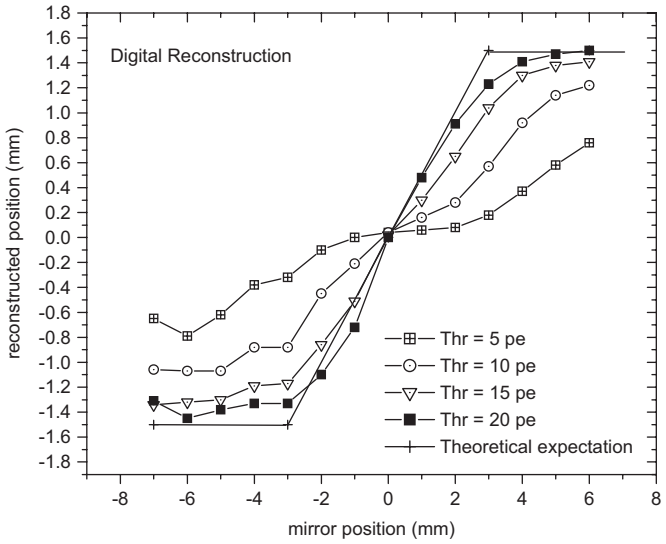

Fig. 9. Scan of the light spot over the two WLS strips at an energy $E_c = 310$ keV converted in the LYSO crystal.

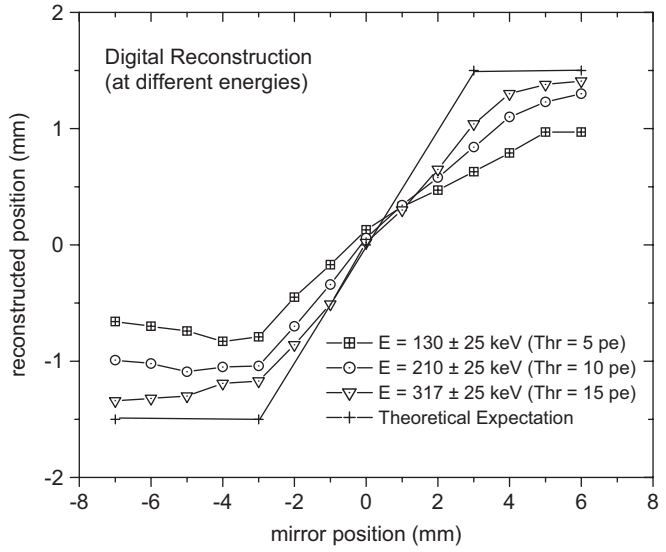

Fig. 10. Scan of the light spot over the two WLS strips at three different energies. The threshold has been set proportional to the converted energy. The z-coordinate is reconstructed digitally.

Fig. 9 shows, as example of the measurements, the reconstructions obtained for a scan orthogonal to the strips at a mean energy $E_c = 310 \pm 32$ keV and a set of discrimination thresholds equivalent to 5, 10, 15 and 20 photoelectrons, respectively.

The deviations with respect to the expected reconstruction shown on the figure, especially outside the interval covered by the strips ($-3 < z_{mir} < 3$ mm), are dependent on the discrimination threshold. Since both strips are more frequently hit when decreasing the discrimination threshold, the mean value of the distributions is consequently forced towards $z_{rec} = 0$. This is an artificial bias due to the limitation to two strips only and will not be present in a module with more strips.

These observations suggest, however, that a discrimination threshold proportional to the energy converted in the LYSO bars would improve the resolution for the reconstruction of Compton interactions. This is illustrated in Fig. 10 which shows the reconstruction obtained at 130, 217 and 310 keV with a discrimination threshold set to 5, 10 and 15 photoelectrons, respectively, so that the detection efficiency (1 and 2 hit strips) during the scan remains higher than 95%. The observed deviations, averaged over the z-range of the strips, are 0.4, 0.3 and 0.15 mm, respectively. Again, this systematic effect is expected to disappear with a larger number of strips.

3.3.2. Analog z-reconstruction

The z-coordinate was reconstructed with the relation

$$z_{rec} = a + b(Q_1 - Q_2)/(Q_1 + Q_2) \quad (8)$$

where a and b are parameters adjusted once.

Fig. 11 displays the results obtained for the same three energies (130, 217 and 310 keV) previously discussed for the digital reconstruction.

As expected, the analog reconstruction of the z-coordinate is in first-order independent of the converted energy. The deviations observed with respect to the "ideal" reconstruction are again due to the limited number of readout strips.

The resolution σ_z scales with $1/\sqrt{E}$ as it was already demonstrated in an earlier publication [2] were PMTs were used as photon detectors. An extrapolation to 511 keV of the resolutions measured at $z_{mir} = 0$ (in between the strips) leads to a value $\sigma_z = 1.2$ mm while the MC simulation predicts ~1 mm but for four readout WLS-strips instead of two. The same MC simulation predicts a resolution $\sigma_z = 0.6$ mm for 511 keV γ rays absorbed nearly uniformly in the depth (3.2 mm) of the crystal bars.

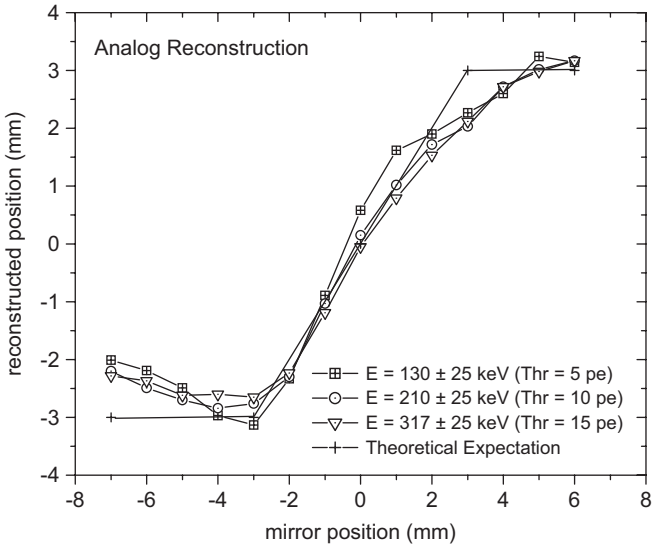

Fig. 11. Scan of the light spot over the two WLS strips at three different energies. The threshold has been set proportional to the converted energy. The z-coordinate in an analog way (see Eq. (8)).

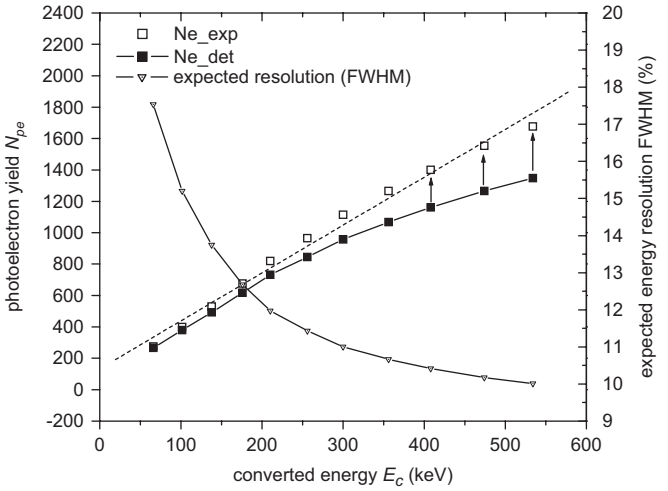

Fig. 12. LYSO bar with MPPC readout. The plot shows the number of detected photoelectrons, as measured, and after a correction for the occupancy of the micro-pixels of the MPPC. The latter are described in good approximation by a straight line fit. The expected energy resolution is derived directly from the measured N_{pe}.

3.4. Photoelectric yield and energy resolution of a LYSO crystal bar with MPPC readout

In a modified set-up a LYSO crystal bar was read out at one end with a MPPC. Standard optical grease was used at the interface. The opposite end was not read, but as before left with its reflective aluminum coating. The energy range of the electron source was increased such that a range from $E_c = 66$–$534\,\text{keV}$ could be measured. The number of detected photoelectrons was again derived from the ADC spectrum. The data are shown in Fig. 12. The polynomial fit (second order) to the data predict for $E_c = 511\,\text{keV}$ a photoelectron yield of $N_{pe} = 1317$. Above $N_{pe} = 600$ the non-linearity of the MPPC due to the limited number of cells ($N_{cell} = 3600$) becomes apparent. The data can be corrected for this combinatorial saturation effect and can then in good approximation be described by a linear fit.

The expected energy resolution, which is also shown in Fig. 12, has been derived from the data using the formula

$$\Delta E/E(\text{FWHM}) = 2.35/\sqrt{N^*_{pe}} \oplus (\Delta E/E)_{intr.} \quad (9)$$

The quantity N^*_{pe} is the number of detected photoelectrons after subtracting 20% cross-talk. The intrinsic resolution of LYSO $(\Delta E/E)_{intr.}$ is 7% [8]. The expected resolution at $E_c = 511\,\text{keV}$ is close to 10% (FWHM) and therefore even slightly better than our previous direct measurement with a ^{22}Na source [2].

4. Conclusions

A set-up of two LYSO crystals and two WLS strips, positioned orthogonally under the LYSO bars, was used to determine the light yield from the WLS strips readout by Hamamatsu MPPCs, type S 10362-33-050C. The LYSO crystals were illuminated by a pulsed and tunable, low-energy electron beam, which allows in a controlled way to create scintillation photons in the crystal equivalent to the absorption of 100–350 keV photons. The light yield at an equivalent energy of 511 keV was determined by extrapolation to be 85 p.e. The resulting axial spatial resolution was determined to be 1.9 mm FWHM at 511 keV for digital coordinate reconstruction and 2.8 mm FWHM for analog reconstruction. These values can be improved in a bigger setup with many LYSO crystals and WLS strip arrays.

We are at present building two modules of 36 LYSO crystals ($3.2 \times 3.2 \times 100\,\text{mm}^3$) each with about 200 WLS strips placed in the gaps of the LYSO stack (4 mm pitch). Both LYSO bars and WLS strips will be read out with tailor-made G-APD devices of dimensions 3.2×3.2 and $3 \times 1.2\,\text{mm}^2$, respectively, under production by ITC-IRST.[10] This will allow in the near future to assemble a demonstrator set-up for a full study of sensitivity and spatial and energy resolution of an axial 3-D PET.

Acknowledgments

We would like to thank our technical staff, C. David, A. Folley, M. van Stenis (CERN), L. Dell'Olio and G. De Carne (INFN Bari) for their excellent work in the preparation of the mechanical and optical components used in the tests.

References

[1] J. Séguinot, et al., Il Nuovo Cimento C 29 (04) (2005) 429.
[2] A. Braem, et al., Nucl. Instr. and Meth. A 580 (2007) 1513.
[3] E.H. Darlington, J. Phys. D 8 (1975) 85.
[4] W.W. Moses, Nucl. Instr. and Meth. A 487 (2002) 123.
[5] I. Vilardi, et al., Nucl. Instr. and Meth. A 564 (2006) 506.
[6] A. Braem, et al., Nucl. Instr. and Meth. A 570 (2007) 467.
[7] A. Braem, et al., Nucl. Instr. and Meth. A 571 (2007) 419.
[8] C.M. Pepin, et al., IEEE Trans. Nucl. Sci. 51 (3) (2004) 789.

[10] Center for Scientific and Technological Research ITC-IRST, Povo (Trento), Italy.